International Journal of Pharmaceutics 472 (2014) 185–191

Contents lists available at ScienceDirect

International Journal of Pharmaceutics

journal homepage: www.elsevier.com/locate/ijpharm

Pharmaceutical nanotechnology

Stabilisation of amorphous ibuprofen in Upsalite, a mesoporous magnesium carbonate, as an approach to increasing the aqueous solubility of poorly soluble drugs

Peng Zhang [a], Johan Forsgren [a], Maria Strømme [a,b,*]

[a] Division for Nanotechnology and Functional Materials, Department for Engineering Sciences, P.O. Box 534, SE-751 21 Uppsala, Sweden
[b] Science for Life Laboratory, Uppsala University, P.O. Box 534, SE-751 21 Uppsala, Sweden

ARTICLE INFO

Article history:
Received 2 May 2014
Received in revised form 13 June 2014
Accepted 14 June 2014
Available online 17 June 2014

Keywords:
Mesoporous
Magnesium carbonate
Poorly soluble drug
Bioavailability
Ibuprofen

ABSTRACT

One attractive approach to increase the aqueous solubility and thus the bioavailability of poorly soluble drugs is to formulate them in their amorphous state since amorphous compounds generally exhibit higher apparent solubilities than their crystalline counterparts. In the current work, mesoporous magnesium carbonate was used to stabilise the amorphous state of the model substance ibuprofen. Crystallisation of the drug was completely supressed in the formulation, resulting in both a higher apparent solubility and a three times faster dissolution rate of the drug where the drug release was shown to be diffusion controlled. It was also shown that the formulation is stable for at least three months when stored at 75% relative humidity. The simple synthesis together with a high loading capacity and narrow pore size distribution of the mesoporous magnesium carbonate is foreseen to offer great advantages in formulations of poorly soluble drugs.

1. Introduction

Over recent decades, the poor aqueous solubility of many active pharmaceutical ingredients (APIs) has been one of the most challenging issues for the pharmaceutical industry. About 40% of newly marketed drugs have poor solubility and 80–90% of drug candidates in the R&D pipeline fail because of solubility problems (Babu and Nangia, 2011; Jia, 2005; Serajuddin, 1999). These drugs with poor aqueous solubility subsequently have low bioavailability, which can limit their therapeutic efficacy. To circumvent this problem, a number of different strategies have been developed, including crystalline salt formulations, API particle reduction, use of solubilisers, co-ground mixtures, and pro-drugs (Brouwers et al., 2009). The success of a formulation strategy depends on both the chemical nature of the drug and practical processing issues. For example, strongly acidic and basic substances can be formulated as salts while weak acids and bases cannot, whereas reduction of the API particle size can lead to build-up of static charges imposing handling difficulties for certain substances (He, 2009).

Since a high number of therapeutically promising, poorly soluble APIs never reach the patient due to lack of suitable formulation methods, there is still a high unmet need for new strategies in this area. One recently embarked on, and seemingly attractive, approach is to stabilise such APIs in their amorphous state since, despite the higher energy and metastability associated with this state, amorphous drugs generally exhibit higher apparent solubility than the crystalline form of the same substance (Brouwers et al., 2009; Galia et al., 1998; Xu et al., 2013). However, because of their metastable nature, amorphous APIs are driven by thermodynamics to crystallise, depending on factors like the glass transition temperature (T_g) and moisture content of the formulation (Yoshioka and Aso, 2007). Thus, the amorphous API needs to be stabilised in the formulation in order to prevent crystallisation. Typically, organic polymers like polyethylene glycol (PEG) and polyvinyl pyrroline (PVP) are used in solid dispersions for this purpose. The complex polymer network acts by reducing the mobility of the drug molecules (Konno et al., 2008; Rawlinson et al., 2007). However, this approach is associated with difficulties in the industrial manufacturing processes and problems with the chemical stability of the products (Qian et al., 2010; Taylor and Zografi, 1997).

Nonetheless, the emergence of nanotechnology in the last decades has provided novel solutions for drug delivery in most

* Corresponding author at: The Ångström Laboratory, Uppsala University, P.O. Box 534, Uppsala SE-751 21, Sweden. Tel.: +46 18 4717231.
E-mail addresses: peng.zhang@angstrom.uu.se (P. Zhang), johan.forsgren@angstrom.uu.se (J. Forsgren), maria.stromme@angstrom.uu.se (M. Strømme).

http://dx.doi.org/10.1016/j.ijpharm.2014.06.025

pharmaceutical formulation areas (Fadeel et al., 2010; Mihranyan et al., 2012), including the area targeting the stabilisation of amorphous APIs. It has been found that mesoporous structures (with pore diameters between 2 and 50 nm) are able to effectively suppress the crystallisation of amorphous substances via geometrical constraints, and also as a result of changes in nucleation mechanisms and kinetics inside the small pores and the interaction between the API and the pore walls (Rengarajan et al., 2008), which can induce a crystalline-to-amorphous phase transformation (Qian and Bogner, 2011). This effect is more pronounced on surfaces featuring high curvature and on those with permanent dipoles, which can induce polarization or form dipole–dipole interactions (Qian et al., 2011). The phenomenon was first observed in 1984 when Nakai et al. (Nakai et al., 1984) saw an anomaly in the melting endotherm and the X-ray diffraction pattern of organic compounds that were mixed together with controlled-pore glass beads. It was suggested that this anomaly was due to amorphisation of the organic molecules under study (i.e. benzoic acid), which had diffused into the voids between the glass beads and existed there in an amorphous state. It was later shown that this type of amorphisation is pronounced in pores with diameters smaller than 50 nm (Nakai et al., 1989). In 2001, the mesoporous silica MCM-41 was proposed as a drug delivery vehicle (Vallet-Regi et al., 2001) and since then different mesoporous silicas have been found useful for improving the solubility of several pharmaceutical compounds (such as itraconazole, atazanavir and ibuprofen (Bras et al., 2011; Heikkila et al., 2007; Mellaerts et al., 2007; Xia et al., 2012)) because of conservation of the amorphous state of the incorporated API. Recent publications have also shown good correlations between improved in vitro solubility and improvements in the bioavailability of drugs formulated in mesoporous materials (Wang et al., 2012; Xia et al., 2012). However, the mesoporous silica industry struggles with high manufacturing costs due to expensive silica sources and surfactants used in the fabrication, as well as environmental concerns related to the often toxic surfactants needed as pore-forming templates in the synthesis (Gerardin et al., 2013). Mesoporous silica is not yet available in bulk quantities and the price for MCM-41 available via e.g. Sigma–Aldrich is presently ~20,000 € kg^{-1} (2014)[1]. Mesoporous silicon produced via etching of crystalline silicon also appears to conserve amorphous APIs, but this type of material is also associated with high production costs and difficulties with large scale manufacturing (Xu et al., 2013).

In connection to the above, it should be pointed out that the mesoporous forms of silica and silicon should not be confused with colloidal silica based on aggregated nanoparticles forming rather fluffy structures. Whereas the latter is commonly used in pharmaceutical formulations as, e.g. anti-caking agent, adsorbent or disintegrant, it lacks the pore structure of the former and has not been shown to have the ability to work as solubility enhancers of poorly soluble substances.

As an alternative to mesoporous silica, we have recently proposed the use of a mesoporous type of vaterite (calcium carbonate) for the stabilisation of amorphous drugs (Forsgren et al., 2013a). The studied vaterite had a smaller pore volume and less well-defined pore size than mesoporous silica but is already listed as 'generally recognized as safe' (GRAS) by the FDA, and it can be produced from inexpensive raw materials in a simple synthetic process, which makes it an interesting drug stabiliser candidate. Vaterite had a stabilising effect on the incorporated amorphous API, which resulted in higher solubilities and faster dissolution rates for both celecoxib and ketokonazol (Forsgren et al., 2013a). However, the vaterite carrier proved to be unstable when exposed to humidity and complete suppression of crystallisation of the incorporated API was not obtained at higher drug loading levels. Other recent publications also show the possibility of using materials like mesoporous alumina and titanium zirconium oxide for the purpose of stabilising amorphous drugs (Kapoor et al., 2009; Wang et al., 2013), however, the FDA does not list these materials as GRAS, which is expected to complicate the route toward regulatory approval for such materials as pharmaceutical excipients.

Recently, we disclosed the synthesis and characterization of a novel mesoporous type of magnesium carbonate, named Upsalite, which can be synthesised using MgO, methanol and CO_2 as raw materials without using surfactants as pore-forming agents (Forsgren et al., 2013b; Frykstrand et al., 2014). Just like calcium carbonate, magnesium carbonate is also GRAS listed and the current work investigates the ability of Upsalite to enhance the solubility and at the same time provides high loading capacity and stability of poorly soluble APIs. Ibuprofen, a well-known, non-steroidal anti-inflammatory drug with limited aqueous solubility is used as model API in this study.

2. Materials and methods

2.1. Materials

Magnesium oxide (MgO) and ibuprofen (IBU) were obtained from Sigma–Aldrich, Sweden. Methanol and ethanol were purchased from VWR International, Sweden. CO_2 was obtained from AirLiquide, Sweden. All chemicals were used as received.

2.2. Synthesis of Upsalite

Upsalite was synthesised as described previously (Forsgren et al., 2013b; Frykstrand et al., 2014). Briefly, 170 g of MgO and 2.5 L CH_3OH were mixed at 500 rpm in a 5 L Ecoclave pressure reactor from Büchi. The reactor was pressurised with 3 bar CO_2 and the reaction was carried out at 55 °C. After four days, the temperature was lowered to room temperature and the reactor was depressurised. The product was dried at 75 °C in a vacuum oven for three days and then calcined at 250 °C for 6 h. Calcination is needed for complete decomposition of the organic intermediates formed in the reaction carried out in the pressure reactor (Frykstrand et al., 2014). When the calcination is performed at temperatures below 350 °C, magnesium carbonate is formed but at higher temperatures the carbonate will decompose into MgO and CO_2. After calcination, the obtained material was in the shape of white, centimetre sized particles that were grinded down to a smaller particle size using a mortar.

2.3. Drug loading procedure

IBU was incorporated into the Upsalite via a soaking method: 203.2 mg IBU was dissolved in 50 mL ethanol and then 642.7 mg of Upsalite was added to the solution. The mixture was placed on an orbital shaker at 100 rpm at room temperature for 24 h to allow for diffusion of IBU into the Upsalite. Subsequently, the suspension was dried in an oven at 70 °C to evaporate the solvent.

2.4. Characterisation

2.4.1. X-ray powder diffraction (XRD)

XRD analysis was performed with a D5000 diffractometer (40 kV, 40 mA, Siemens/Bruker) using Cu-Kα radiation (λ = 0.154 nm). Samples were ground in a mortar and put on silicon sample holders with zero background prior to analysis.

[1] www.sigmaaldrich.com on 22 Jan 2014.

2.4.2. Fourier transform infrared spectroscopy (FTIR)

FTIR studies were carried out in a Bruker FTS66v/s spectrometer with an attenuated total reflectance (ATR) sample holder. All FTIR spectra were collected at a spectrum resolution of 4 cm^{-1} with 50 scans over a range of 4000–400 cm^{-1}. A background scan was acquired before scanning the samples.

2.4.3. N_2 sorption analysis

Gas sorption isotherms were obtained using an ASAP 2020 from Micromeritics, operated at −196 °C. Prior to analysis, the samples were degassed under vacuum at 90 °C for 12 h. The specific surface area (SSA) was calculated using the multipoint Brunauer–Emmett–Teller (BET) method (Brunauer et al., 1938) for adsorption values in the relative pressure range between 0.05 and 0.3, while the pore size distribution was calculated based on the density functional theory (DFT) method using the model for N_2 at −196 °C. The total pore volume was obtained from single point adsorption at a relative pressure $P/P_0 \approx 1$. These calculations, including calculations of the errors of the SSA values, were all performed using the ASAP 2020 (Micromeritics) software.

2.4.4. Thermal gravimetric analysis (TGA)

TGA was carried out on a Mettler Toledo, model TGA/SDTA851e, under airflow in an inert aluminium cup. The samples were heated from room temperature to 600 °C at a heating rate of 3 °C min^{-1}.

2.4.5. Differential scanning calorimetry (DSC)

DSC was performed on a DSC Q2000 instrument from TA instruments using Exstar software. Samples of 3.5–5.5 mg were weighed into 5 mm aluminium pans and sealed. Samples were first cooled to −35 °C and then heated to 150 °C at a heating rate of 3 °C min^{-1}. The instrument was calibrated for the melting point and heat of fusion (T_m [°C] and ΔH_m [mJ mg^{-1}]) of indium (156.6 °C and 28.4 mJ mg^{-1}).

2.4.6. Scanning electron microscopy (SEM)

SEM imaging of the Upsalite was performed with a Leo 1550 FEG microscope (Zeiss, Oberkochen, Germany) equipped with an in-lens detector. A thin gold/palladium layer was sputtered onto samples prior to analysis to avoid charging of the samples. The analysis was performed at 1.5 kV acceleration voltage.

2.4.7. Drug-release measurement

The release of IBU was measured in a USP-2 dissolution bath (Sotax AT7 Smart, Sotax AG, Switzerland) equipped with 1000 mL vessels (37 °C, 50 rpm). Samples with a total drug content of 17.5 mg IBU were placed in vessels containing 500 mL phosphate buffer (pH 6.8). Aliquots of 3 mL were withdrawn from each vessel at regular intervals for 125 min and the drug concentration in the liquid samples was analysed using UV/visual absorbance spectroscopy at 219.4 nm (1650PC, Shimadzu Corporation, Kyoto, Japan). Measurements were made in triplicates on pure IBU crystals and IBU-loaded Upsalite (Upsalite-IBU) and the mean concentration values and corresponding standard deviations were calculated.

2.4.8. Long-term stability test

An amount of the Upsalite-IBU sample was stored in a desiccator at room temperature and 75% RH (obtained with a saturated mixture of water and NaCl) for three months. The sample was then analysed with XRD and DSC to investigate whether a humid atmosphere induced crystallisation of the incorporated IBU. Upsalite without IBU was also stored under the same conditions to examine whether the humidity affected the carrier material.

3. Results and discussion

Fig. 1 presents a photograph of the as-synthesised Upsalite particles and SEM images of grounded Upsalite particles. The photograph shows white and millimetre to centimetre-sized

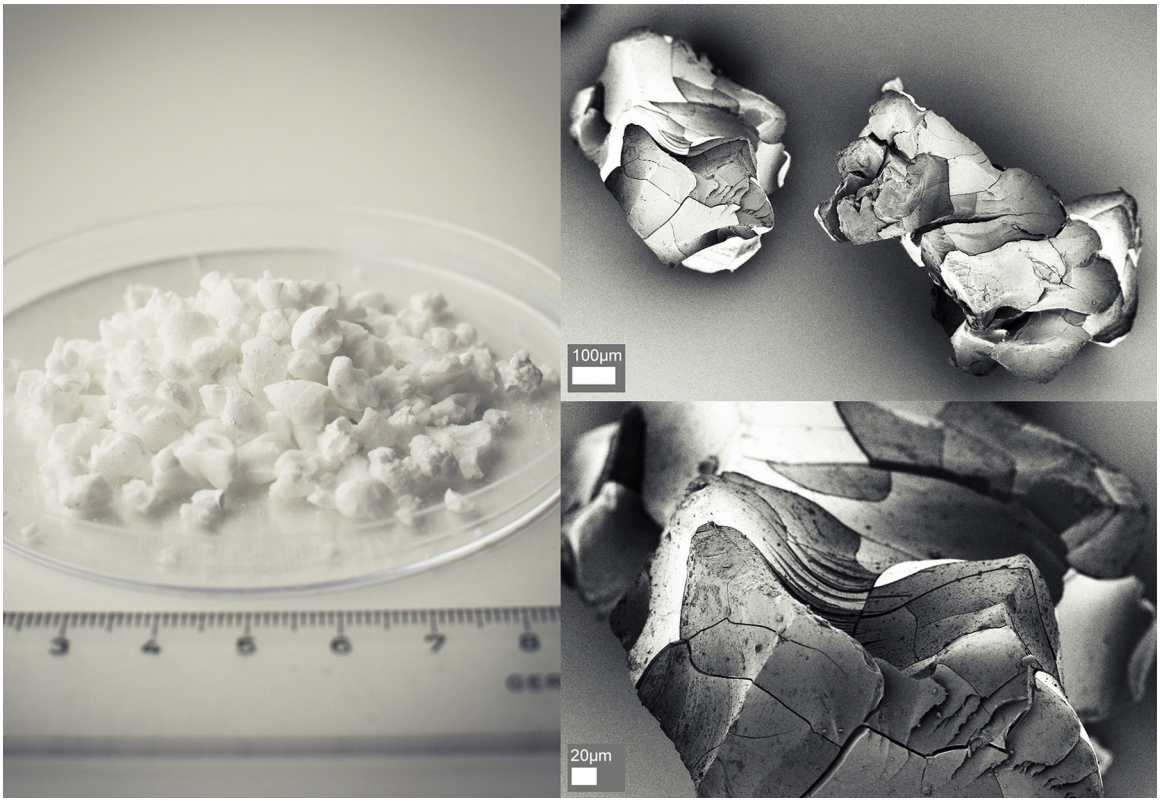

Fig. 1. Left panel: a photograph of the as-synthesised Upsalite. Right panels: SEM images of grinded Upsalite particles.

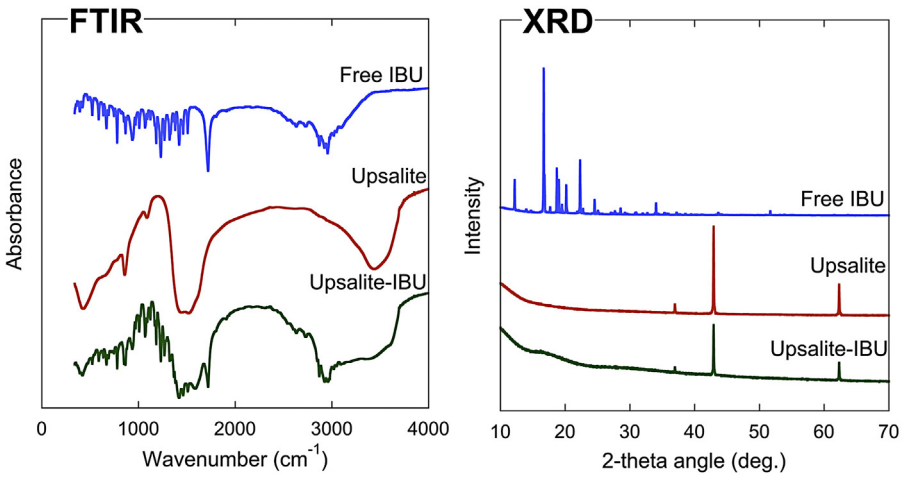

Fig. 2. Left panel: FTIR absorption spectrums for the samples under study. In the spectrum of Upsalite, the three visible bands at ~1440 cm^{-1}, ~1100 cm^{-1} and ~850 cm^{-1} are all due to vibrations of the CO_3 group. Right panel: XRD patterns for the samples under study. The peaks at ~37°, ~43° and ~62° in the Upsalite and Upsalite-IBU samples correspond to unreacted MgO residing in the carbonate structure. The halo at ~15–20° in Upsalite-IBU indicates an amorphous character of the incorporated ibuprofen.

particles of irregular shape typical for the amorphous magnesium carbonate in Upsalite. The SEM images display that whereas grinding reduced the particle size down to a few hundred micrometre, the particle shape remained irregular.

The magnesium carbonate component in Upsalite is evident from the transmission FTIR spectra of the material, see Fig. 2, where bands observed at ~850 cm^{-1}, ~1100 cm^{-1} and ~1400 cm^{-1} correspond to the carbonate group (Raade, 1970) and the absorbance band at ~3440 cm^{-1} corresponds to adsorbed water. No new absorbance bands were observed for the Upsalite-IBU sample in addition to those present in the spectra from the free IBU and the empty Upsalite samples, which indicate that the IBU in Upsalite was physisorbed rather than chemisorbed to the surface of the pore walls in Upsalite.

Fig. 2 also displays the XRD patterns for Upsalite obtained after calcination as well as for free IBU and Upsalite-IBU. The peaks in the XRD patterns for Upsalite and Upsalite-IBU correspond to unreacted MgO (Forsgren et al., 2013b). The lack of other peaks in these samples shows that the magnesium carbonate component in Upsalite is amorphous, in agreement with previous studies (Forsgren et al., 2013b; Frykstrand et al., 2014; Pochard et al., 2014), and also that the IBU incorporated in the Upsalite-IBU sample is amorphous.

The lack of crystalline IBU in the Upsalite-IBU sample was also evident from the DSC curves displayed in Fig. 3. The endothermic event at 78 °C for the free IBU corresponds to the melting point for the crystalline structure. The complete lack of an endothermic event at the same temperature for the Upsalite-IBU sample confirms that the incorporated IBU was not present in a crystalline state inside the pores. No peaks corresponding to any endo- or exothermic events were detected in the DSC scan between −35 °C and 150 °C for the Upsalite-IBU sample. The XRD and DSC data prove that the mesoporous structure in Upsalite completely suppresses crystallisation of the incorporated IBU. Further, since there were no signs of crystalline IBU in the Upsalite-IBU sample, it can be concluded that only an insignificant, if any, amount of IBU resides on the outer surface of the carrier particles. The outer surface area of the carrier particles is negligible compared to the internal surface area and only has a limited ability to interact with the IBU and thus suppress crystallisation of the substance. This result stands in contrasts to studies on mesoporous silica where crystalline ibuprofen is found on the surface on the particles when the drug loading is carried out using similar impregnation methods (Bras et al., 2011; Shen et al., 2010; Szegedi et al., 2012). Hence, the Upsalite displays a superior ability to adsorb ibuprofen into the porous structure or the particles.

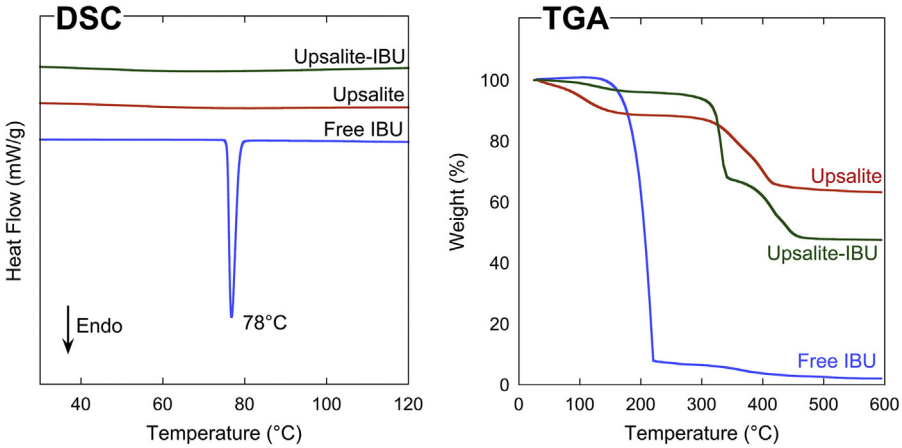

Fig. 3. Left panel: DSC curves for the studied samples. The absence of a melting peak for the Upsalite-IBU sample shows that the incorporated IBU lacks a lattice energy associated with a crystalline structure, hence, the IBU is in an amorphous state. Right panel: TGA curves for the studied samples.

No signs of crystallisation of the IBU incorporated in Upsalite were detected with XRD and DSC stability testing after the sample had been stored at 75% RH for three months at room temperature. Nor were there any signs of crystallisation of the amorphous magnesium carbonate component in the Upsalite after exposure to the humid atmosphere. This indicates good stability for the proposed formulation, even under tough conditions, since moisture is a well-known plasticiser of pharmaceutical formulations and adsorbed water can decrease the T_g of many formulations and allow sufficient drug molecule mobility to induce crystallisation of amorphous drugs (Ahlneck and Zografi, 1990; Andronis et al., 1997; Qian et al., 2012).

After loading Upsalite with IBU, TGA was carried out to investigate the degree of drug loading in the carrier. The TGA curves for Upsalite, free IBU and Upsalite-IBU are presented in Fig. 3. As evident from the figure, free IBU evaporated at ~200 °C while the magnesium carbonate in Upsalite decomposed into MgO and CO_2 at ~370 °C. Two distinct regions of weight loss, at ~330 °C and ~420 °C, were observed for the Upsalite-IBU sample; the first, clearly associated with the evaporation of IBU, corresponds exactly to the 24 wt% of IBU used in the preparation of the sample and the second with the decomposition of the magnesium carbonate. Interestingly, the evaporation temperature for the incorporated IBU was increased by about 140 °C compared to the free substance. A similar phenomenon has been observed previously for IBU as well as for ketoprofen incorporated in mesoporous materials (Hillerstrom et al., 2009; Li-Hong et al., 2013; Moritz and Laniecki, 2012; Wang et al., 2006). The increase in evaporation temperature could be explained by capillary forces in the pores, as described by the Kelvin equation:

$$\ln\frac{P}{P_0(T)} = -\frac{2\gamma}{R_K}\frac{V_M}{RT} \quad (1)$$

where P is the equilibrium vapour pressure, $P_0(T)$ is the saturation vapour pressure at the given temperature, γ is the surface tension, V_M is the molar volume of the liquid, R_K is the Kelvin radius of the liquid curvature and R is the universal gas constant. According to the Kelvin equation, lower pressures or higher temperatures are needed to evaporate liquids from nanometre-sized pores compared to a free liquid; this is a result of capillary forces acting on the liquid and forcing it to remain in a condensed state in the pores, leading to the increased evaporation temperature for the incorporated IBU.

The pore volume and SSA of the studied samples are given in Table 1 while the pore size distributions obtained from the N_2 sorption analysis are displayed in Fig. 4. Both SSA and pore size distribution of unloaded samples are similar to those measured previously for calcined Upsalite (Frykstrand et al., 2014). From the figure and the table, respectively, it is evident that the pore diameter in the Upsalite-IBU sample was reduced by about 2 nm compared to the unloaded Upsalite whereas the pore volume was reduced to half. Since the diameter of an IBU molecule is about 1 nm (Vallet-Regi et al., 2001), this indicates that the IBU molecules were arranged in a monolayer along the pore walls of Upsalite rather than in clustered multilayer structures. The pore volume data also suggest that the 24 wt% IBU loading degree was about half

Table 1
Specific surface area (SSA) and total pore volume (V_{pore}) of the Upsalite samples.

Sample	SSA ($m^2\,g^{-1}$)	V_{pore} ($cm^3\,g^{-1}$)
Upsalite	349 ± 0.63[a]	0.83
Upsalite-IBU	245 ± 1.17[a]	0.39

[a] The values are based on single measurements and the errors were obtained using the ASAP 2020 (Micromeritics) software.

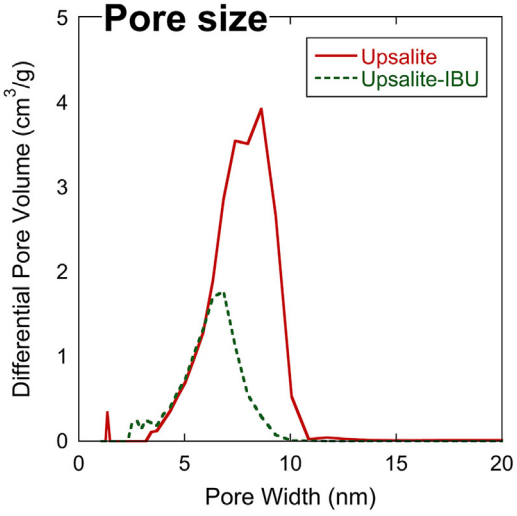

Fig. 4. Pore size distributions for the empty and the IBU-filled Upsalite.

of the maximum drug loading capacity of Upsalite. More drug is expected to enter the carrier particles if the amount of drug employed in the loading procedure is increased or if other loading techniques are employed; such as spray drying which has been shown to improve the loading capacity of mesoporous silica (Shen et al., 2010).

The dissolution profiles of free IBU and IBU incorporated in Upsalite are shown in Fig. 5. Clearly, the dissolution of the amorphous IBU inside Upsalite was more rapid than that of the free substance. During the first 5 min, the dissolution rate for the IBU in the Upsalite-IBU sample was three times higher than that for the free substance; similarly, 50% of the IBU was dissolved and released from the Upsalite carrier within 12 min while it took 30 min for the free substance to reach the same dissolution level. The dissolution of IBU in its free form levelled out at ~75% after about 80 min, corresponding to a concentration of IBU in the dissolution media of 27 mg L^{-1}. In contrast, the dissolution of the amorphous IBU from Upsalite continued beyond 85%, corresponding to a concentration of 30 mg L^{-1} IBU. This shows that the apparent solubility of the drug could be increased by at least 11% under the given conditions when it was formulated with Upsalite. One way Anova analysis gave that this difference was significant at $p < 0.05$ level [$F(1,4) = 22.4$, $p = 0.009$]. However, in the present study, the amount of drug used in the release experiments was close to the solubility limit of free ibuprofen under the given conditions and an even higher supersaturated state of the drug is expected if a larger amount of sample is used. This will be investigated in future studies. In order to examine the release mechanism of IBU from the Upsalite particles, the release data was fitted with the semi-empirical Korsmeyer–Peppas equation:

$$\frac{M_t}{M_\infty} = kt^n \quad (2)$$

where M_t/M_∞ is the released fraction of the drug, k is a kinetic constant, t is the release time and n is the diffusional exponent characteristic of the release mechanism. The Korsmeyer–Peppas equation is valid for the first 60% of the released amount of drug and can be used to analyse the release mechanism from non-swelling and swelling matrices (Ritger and Peppas, 1987a,b,b). For non-swelling systems it can be used to discriminate between Fickian diffusion, non-Fickian (anomalous) transport and zero-order release mechanisms: for a monodisperse sample of spherical particles, an n-value of 0.43 represents purely Fickian diffusion

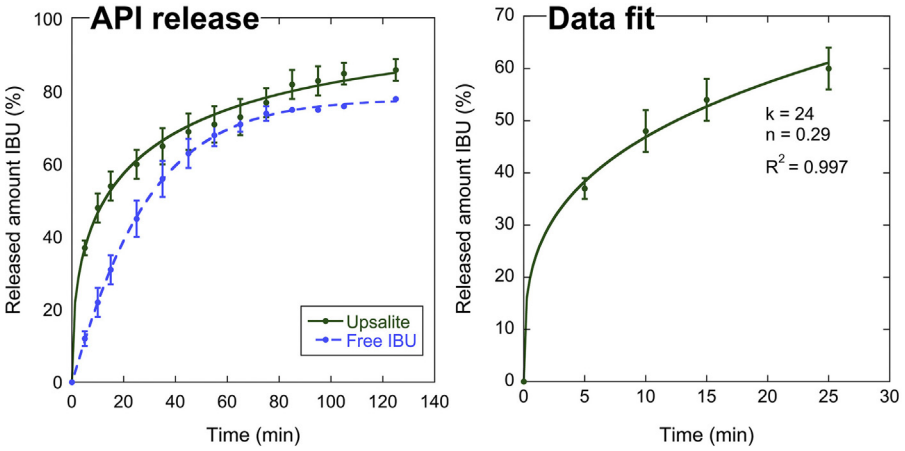

Fig. 5. Left panel: IBU dissolution profiles for free IBU and IBU incorporated in Upsalite. Right panel: the initial 60% of IBU released from the Upsalite-IBU sample fitted to the Korsmeyer–Peppas equation $M_t/M_\infty = kt^n$. The obtained fitting parameters are displayed. All measurements were made in triplicates and the data is displayed as the mean values with corresponding standard deviation.

while an n-value of 1.0 represents a zero-order release mechanism. Any n-value between 0.43 and 1.0 represents some type of combination of release mechanisms or non-Fickian transport (Ritger and Peppas, 1987a). Since the Upsalite particles of the current work have been grinded and the aspect ratio, as determined from the SEM images, is fairly low the particles can be regarded as spherical. When the release data for the Upsalite-IBU sample was fitted with the Korsmeyer–Peppas equation, it showed good correlation ($R^2 > 0.99$) and an n-value of 0.29 was obtained, see Fig. 5. This behaviour witnesses of a release mechanism that is exclusively diffusion limited from particles with a wide size distribution (Ritger and Peppas, 1987a). The wide particle distribution is expected since the Upsalite particles were not sieved after grinding. In the future, it would thus be of interest to investigate the release of various substances from samples with well-defined particle sizes to analyse how the release time can be tailored by controlling the particle size.

4. Conclusions

As evident from the current work, the mesoporous magnesium carbonate Upsalite provides a great potential for the development of new drug formulations of APIs with poor aqueous solubility. Crystallisation of the BCS class II substance ibuprofen was completely suppressed by the mesoporous structure of Upsalite, leading to both faster dissolution rate and increased solubility compared to the crystalline drug in free form, and the formulation was stable for at least three months when stored at 75% relative humidity. The easy fabrication of Upsalite and the fact that its constituent magnesium carbonate is already GRAS-listed are expected to offer advantages in the considered application area compared to e.g. mesoporous silica and mesoporous silicon, while the stability and drug loading capacity of the material are superior to those previously evaluated mesoporous vaterite (calcium carbonate). The diffusion limited release of the incorporated substance provides means to control the release rate by adjusting the particle size of the carrier particles, something that will be investigated in future works.

Acknowledgements

Assoc. Prof. Albert Mihranyan is gratefully acknowledged for fruitful discussions regarding the drug release results. We acknowledge the funding agency Vinnova as well as the Carl Trygger Foundation and the China Scholarship Council (CSC) for financial support of the presented work. The DSC measurements were performed on resources provided by the BioMat platform at SciLifeLab, Uppsala. The funding sources had no involvement in the collection, analysis and interpretation of data; in the writing of the report; or in the decision to submit the article for publication.

References

Ahlneck, C., Zografi, G., 1990. The molecular-basis of moisture effects on the physical and chemical-stability of drugs in the solid-state. Int. J. Pharm. 62, 87–95.
Andronis, V., Yoshioka, M., Zografi, G., 1997. Effects of sorbed water on the crystallization of indomethacin from the amorphous state. J. Pharm. Pharm. Sci. 86, 346–351.
Babu, N.J., Nangia, A., 2011. Solubility advantage of amorphous drugs and pharmaceutical cocrystals. Cryst. Growth Des. 11, 2662–2679.
Bras, A.R., Merino, E.G., Neves, P.D., Fonseca, I.M., Dionisio, M., Schonhals, A., Correia, N.T., 2011. Amorphous ibuprofen confined in nanostructured silica materials: a dynamical approach. J. Phys. Chem. C 115, 4616–4623.
Brouwers, J., Brewster, M.E., Augustijns, P., 2009. Supersaturating drug delivery systems: the answer to solubility-limited oral bioavailability? J. Pharm. Pharm. Sci. 98, 2549–2572.
Brunauer, S., Emmett, P.H., Teller, E., 1938. Adsorption of gases in multimolecular layers. J. Am. Chem. Soc. 60, 309–319.
Fadeel, B., Kasemo, B., Malmsten, M., Strømme, M., 2010. Nanomedicine: reshaping clinical practice. J. Intern. Med. 267, 2–8.
Forsgren, J., Andersson, M., Nilsson, P., Mihranyan, A., 2013a. Mesoporous calcium carbonate as a phase stabilizer of amorphous celecoxib – an approach to increase the bioavailability of poorly soluble pharmaceutical substances. Adv. Healthcare Mater. 2, 1469–1476.
Forsgren, J., Frykstrand, S., Grandfield, K., Mihranyan, A., Strømme, M., 2013b. A template-free, ultra-adsorbing, high surface area carbonate nanostructure. PLoS One 8, e68486.
Frykstrand, S., Forsgren, J., Mihranyan, A., Strømme, M., 2014. On the pore forming mechanism of Upsalite, a micro- and mesoporous magnesium carbonate. Microporous Mesoporous Mater. 190, 99–104.
Galia, E., Nicolaides, E., Horter, D., Lobenberg, R., Reppas, C., Dressman, J.B., 1998. Evaluation of various dissolution media for predicting in vivo performance of class I and II drugs. Pharm. Res. 15, 698–705.
Gerardin, C., Reboul, J., Bonne, M., Lebeau, B., 2013. Ecodesign of ordered mesoporous silica materials. Chem. Soc. Rev. 42, 4217–4255.
He, X., 2009. Integration of physical, chemical, mechanical, and biopharmaceutical properties in solid oral dosage form development. In: Qiu, Y., Chen, Y., Zhang, G. G.Z., Liu, L., Porter, W.R. (Eds.), Developing Solid Oral Dosage Forms. Academic Press, San Diego pp. 407, 409–441.
Heikkila, T., Salonen, J., Tuura, J., Hamdy, M.S., Mul, G., Kumar, N., Salmi, T., Murzin, D. Y., Laitinen, L., Kaukonen, A.M., Hirvonen, J., Lehto, V.P., 2007. Mesoporous silica material TUD-1 as a drug delivery system. Int. J. Pharm. 331, 133–138.
Hillerstrom, A., van Stam, J., Andersson, M., 2009. Ibuprofen loading into mesostructured silica using liquid carbon dioxide as a solvent. Green Chem. 11, 662–667.
Jia, L., 2005. Nanoparticle formulation increases oral bioavailability of poorly soluble drugs: approaches, experimental evidences and theory. Curr. Nanosci. 1, 237–243.

Kapoor, S., Hegde, R., Bhattacharyya, A.J., 2009. Influence of surface chemistry of mesoporous alumina with wide pore distribution on controlled drug release. J. Control. Release 140, 34–39.
Konno, H., Handa, T., Alonzo, D.E., Taylor, L.S., 2008. Effect of polymer type on the dissolution profile of amorphous solid dispersions containing felodipine. Eur. J. Pharm. Biopharm. 70, 493–499.
Li-Hong, W., Xin, C., Hui, X., Li-Li, Z., Jing, H., Mei-Juan, Z., Jie, L., Yi, L., Jin-Wen, L., Wei, Z., Gang, C., 2013. A novel strategy to design sustained-release poorly water-soluble drug mesoporous silica microparticles based on supercritical fluid technique. Int. J. Pharm. 454, 135–142.
Mellaerts, R., Aerts, C.A., Van Humbeeck, J., Augustijns, P., Van den Mooter, G., Martens, J.A., 2007. Enhanced release of itraconazole from ordered mesoporous SBA-15 silica materials. Chem. Commun. 1375–1377.
Mihranyan, A., Ferraz, N., Strømme, M., 2012. Current status and future prospects of nanotechnology in cosmetics. Prog. Mater. Sci. 57, 875–910.
Moritz, M., Laniecki, M., 2012. SBA-15 mesoporous material modified with APTES as the carrier for 2-(3-benzoylphenyl)propionic acid. Appl. Surf. Sci. 258, 7523–7529.
Nakai, Y., Yamamoto, K., Terada, K., Ichikawa, J., 1984. Interaction of medicinals and porous powder. I. Anomalous thermal behavior of porous glass mixtures. Chem. Pharm. Bull. 32, 4566–4571.
Nakai, Y., Yamamoto, K., Izumikawa, S., 1989. Interaction of medicinals and porous powder. 3. Effects of pore diameter of porous-glass powder on crystalline properties. Chem. Pharm. Bull. 37, 435–438.
Pochard, I., Frykstrand, S., Ahlström, O., Forsgren, J., Strømme, M., 2014. Water and ion transport in ultra-adsorbing porous magnesium carbonate studied by dielectric spectroscopy. J. Appl. Phys. 115, 044306.
Qian, F., Huang, J., Hussain, M.A., 2010. Drug-polymer solubility and miscibility: stability consideration and practical challenges in amorphous solid dispersion development. J. Pharm. Pharm. Sci. 99, 2941–2947.
Qian, K.K., Bogner, R.H., 2011. Spontaneous crystalline-to-amorphous phase transformation of organic or medicinal compounds in the presence of porous media, part 1: thermodynamics of spontaneous amorphization. J. Pharm. Pharm. Sci. 100, 2801–2815.
Qian, K.K., Suib, S.L., Bogner, R.H., 2011. Spontaneous crystalline-to-amorphous phase transformation of organic or medicinal compounds in the presence of porous media, part 2: amorphization capacity and mechanisms of interaction. J. Pharm. Pharm. Sci. 100, 4674–4686.
Qian, K.K., Wurster, D.E., Bogner, R.H., 2012. Spontaneous crystalline-to-amorphous phase transformation of organic or medicinal compounds in the presence of porous media, part 3: effect of moisture. Pharm. Res. 29, 2698–2709.
Raade, G., 1970. Dypingite, a new hydrous basic carbonate of magnesium, from Norway. Am. Mineral. 55, 1457–1465.
Rawlinson, C.F., Williams, A.C., Timmins, P., Grimsey, I., 2007. Polymer-mediated disruption of drug crystallinity. Int. J. Pharm. 336, 42–48.
Rengarajan, G.T., Enke, D., Steinhart, M., Beiner, M., 2008. Stabilization of the amorphous state of pharmaceuticals in nanopores. J. Mater. Chem. 18, 2537–2539.
Ritger, P.L., Peppas, N.A., 1987a. A simple equation for description of solute release. I. Fickian and non-fickian release from non-swellable devices in the form of slabs, spheres, cylinders or discs. J. Control. Release 5, 23–36.
Ritger, P.L., Peppas, N.A., 1987b. A simple equation for description of solute release. II. Fickian and anomalous release from swellable devices. J. Control. Release 5, 37–42.
Serajuddin, A.T.M., 1999. Solid dispersion of poorly water-soluble drugs: early promises, subsequent problems, and recent breakthroughs. J. Pharm. Pharm. Sci. 88, 1058–1066.
Shen, S.C., Ng, W.K., Chia, L., Dong, Y.C., Tan, R.B.H., 2010. Stabilized amorphous state of ibuprofen by co-spray drying with mesoporous SBA-15 to enhance dissolution properties. J. Pharm. Pharm. Sci. 99, 1997–2007.
Szegedi, A., Popova, M., Goshev, I., Klebert, S., Mihaly, J., 2012. Controlled drug release on amine functionalized spherical MCM-41. J. Solid State Chem. 194, 257–263.
Taylor, L.S., Zografi, G., 1997. Spectroscopic characterization of interactions between PVP and indomethacin in amorphous molecular dispersions. Pharm. Res. 14, 1691–1698.
Vallet-Regi, M., Ramila, A., del Real, R.P., Perez-Pariente, J., 2001. A new property of MCM-41: drug delivery system. Chem. Mater. 13, 308–311.
Wang, C.Y., He, C.Y., Tong, Z., Liu, X.X., Ren, B.Y., Zeng, F., 2006. Combination of adsorption by porous $CaCO_3$ microparticles and encapsulation by polyelectrolyte multilayer films for sustained drug delivery. Int. J. Pharm. 308, 160–167.
Wang, Z.H., Chen, B., Quan, G.L., Li, F., Wu, Q.L., Dian, L.H., Dong, Y.X., Li, G., Wu, C.B., 2012. Increasing the oral bioavailability of poorly water-soluble carbamazepine using immediate-release pellets supported on SBA-15 mesoporous silica. Int. J. Nanomed. 7, 5807–5818.
Wang, X.J., Chen, D.H., Cao, L., Li, Y.C., Boyd, B.J., Caruso, R.A., 2013. Mesoporous titanium zirconium oxide nanospheres with potential for drug delivery applications. ACS Appl. Mater. Interfaces 5, 10926–10932.
Xia, X., Zhou, C., Ballell, L., Garcia-Bennett, A.E., 2012. In vivo enhancement in bioavailability of atazanavir in the presence of proton-pump inhibitors using mesoporous materials. ChemMedChem 7, 43–48.
Xu, W.J., Riikonen, J., Lehto, V.P., 2013. Mesoporous systems for poorly soluble drugs. Int. J. Pharm. 453, 181–197.
Yoshioka, S., Aso, Y., 2007. Correlations between molecular mobility and chemical stability during storage of amorphous pharmaceuticals. J. Pharm. Pharm. Sci. 96, 960–981.